Efficiency of terahertz detection in electro-optic polymer sensors with interdigitated coplanar electrodes

Qiang Jiang (蒋 强)[1], Xuan Wang (王 暄)[1*], Yue Wang (王 玥)[2], and Zhiyuan Li (李志远)[1]

[1]*State Key Laboratory Breeding Base of Dielectrics Engineering, Harbin University of Science and Technology, Harbin 150080, China*

[2]*Key Laboratory of Engineering Dielectrics and Its Application, Ministry of Education, Harbin University of Science and Technology, Harbin 150080, China*

[*]*Corresponding author: topix@sina.com*

Received May 21, 2013; accepted July 1, 2013; posted online August 30, 2013

We discuss the efficiency of an electro-optic (EO) polymer sensor with interdigitated coplanar electrodes. The developed EO sensor is used to detect terahertz radiation via EO sampling. Results show that the sensor improves more significantly detection sensitivity than does a sensor with sandwich configurations.

OCIS codes: 230.4320, 230.2090, 040.2235.
doi: 10.3788/COL201311.092301.

All-optical techniques are often used to realize the generation and detection of terahertz (THz) radiation in THz applications. In such techniques, optical rectification[1] is used on electro-optic (EO) materials to generate THz radiation, and EO sampling[2] is carried out to detect THz radiation. Although this method presents good sensitivity and large bandwidths, strong dispersion and absorption gaps associated with the lattice resonance in crystalline EO materials constantly occur. Therefore, a smooth frequency response is difficult to obtain. If such THz sources and detectors are employed in spectroscopic studies, spectral information in the gaps cannot be extracted. Given that EO polymers are used to generate and detect THz radiation[3], the organic EO polymer family has become an ideal alternative to crystalline EO materials for application in THz systems. These materials exhibit higher EO coefficients[4,5], greater coherence length, and more variable processing techniques[6,7] than do their crystalline counterparts. The greatest advantage of using amorphous EO polymer films as THz emitters and sensors is the absence of dispersion or absorption that results from the lattice resonance effect; consequently, a gap-free THz spectrum is created[8].

In using an EO polymer sensor to detect THz radiation, a polymer film is sandwiched between two poling electrodes, which consist of either evaporated gold or a transparent conducting oxide (TCO), such as indium tin oxide (ITO) or TCO-TCO. In an EO polymer sensor with sandwich configurations, the poling direction is normal to the polymer plane. Therefore, the poling direction must be rotated with respect to the incident THz beam, so that an appreciable component of the THz electric field can be aligned with the poled axis of the polymer film. The sensitivity of sandwich configurations generally acts as a function of the incident angle (θ) of THz and probe beams. In this letter, we present the use of EO polymer devices with interdigitated coplanar electrodes as THz radiation sensors. Such devices are ideal because they allow optimal overlap between the THz electric field and the poling direction of the polymer film without an external slant angle. The configurations have been effectively used in other types of systems, such as piezoelectric transducers[9] and photorefractive polymers[10].

EO polymer film sensors for detecting THz radiation have two types of configurations: sandwich configuration and interdigitated coplanar configuration. The former has been described in Ref. [11]. Therefore, only the preparation of the latter is introduced in the current work. The schematic of an EO polymer sensor with interdigitated coplanar electrodes is shown in Fig. 1. The copper-clad printed circuit board includes an embedded interdigitated electrode chip, which is carved on an aluminum evaporated glass substrate by laser micromachining[12]. The electrode area of the sensor has dimensions of 14× 14 (mm). Rounded electrode edges reduce high-field fringing effects, consequently minimizing the occurrence of polymer dielectric breakdown during poling.

The EO polymer material used in this study is a poly(methyl methacrylate) (PMMA) with disperse red 1 (DR1) dye attached as a side chain at a concentration of 10 mol%. The EO polymer (PMMA-DR1) has a glass transition temperature (T_g) of approximately 83 °C, and the UV absorption (λ_{max}) is 467 nm. The chloroform solution of this polymer is first filtrated through a 0.2 μm syringe filter and then spin coated onto the glass substrate with the interdigitated coplanar electrodes. The

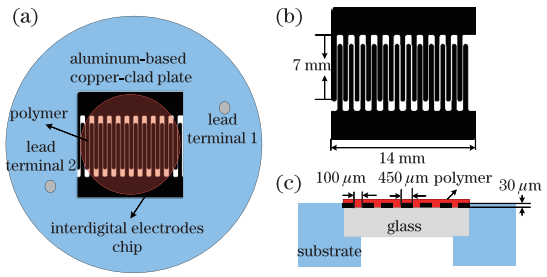

Fig. 1. (Color online) Schematic of the electro-optic polymer sensor with interdigitated coplanar electrodes; (a) and (c) top-down view and cross-section of the sensor, respectively; (b) expanded view of the interdigitated chip (space: 100 μm; width: 450 μm; length: 7 mm; thickness: 30 μm).

devices are then baked in a vacuum oven at 70 °C for 12 h to remove residual solvents. The thickness of the resultant film is controlled at 30 to 100 μm by using appropriate polyimide spacers. The EO polymer sensors on both sandwich and interdigitated coplanar configurations are poled under a unified condition by an applied field of 100 V/μm at T_g. After poling, we carry out ellipsometry[13] to measure the EO coefficients of the films. The EO coefficient (γ_{33}) of PMMA-DR1 is 10.5 pm/V at 1 064 nm. We do not observe significant degradation of the performance of these EO polymer films over the next few weeks.

A schematic of the experimental setup is shown in Fig. 2(a). We used a mode-locked Ti:sapphire laser (Spectra-Physics) as the optical source for generating and detecting THz pulses. The laser oscillator operated at a central wavelength of 800 nm with a repetition rate of 82 MHz produces transform-limited optical pulses at a duration of 50 fs. The optical pump beam, with an average power of 350 mW, is focused onto a 1-mm-thick $<110>$ ZnTe crystal at normal incidence. THz pulses are generated by optical rectification and transmitted through the crystal. The pulses are then collected and focused onto the EO polymer sensor by a pair of off-axis parabolic mirrors. A 200-μm HDPE film is used to block any residual pump beam after THz generation. The polarization state of the 15-mW probe beam is altered from its initial 45° polarization. For THz pulse detection, we employ transmission geometry, as shown schematically in Figs. 2(b) and (c). The corresponding phase retardation is measured with balanced photodiodes in a differential detection scheme[14].

The sensitivity of the EO sampling sensors is directly proportional to the phase retardation induced by an external electric field. When EO sampling is used to detect THz radiation, the external electric field generated by the THz pulses causes a proportional change in the refractive index of the EO medium. A linearly polarized probe beam that simultaneously passes through this medium experiences phase retardation along any component parallel to the THz electric field. This retardation[15] between the s- and p-polarizations of the optical probe beam should be determined. As shown in Fig. 2(b), both the probe beam and THz pulses are incident upon the polymer at an external angle θ. The THz field-induced phase retardation between the two polarizations of the optical probe beam in the sensor with sandwich configurations is expressed by[16]

$$\Delta\Gamma_1 = \frac{2\pi d_p n^3 \gamma_{33}}{3\lambda} \frac{\sin\theta}{(n^2 - \sin\theta)^{\frac{1}{2}}} E_{\mathrm{THz}}, \tag{1}$$

where d_p is the polymer film thickness, γ_{33} is the EO coefficient of the polymer, n is the refractive index, and λ is the wavelength of the probe beam. The poling direction of the sensor with interdigitated coplanar configurations is parallel to the polymer surface (Fig. 2(c)). This parallelity enables the THz electric field to be fully projected onto the poling axis under normal incidence. If the electrode spacing (d_s) is assumed to be constant, then the optical path difference of the probe beam in the proposed sensor is

$$l_p - l_s = d_s(n_e - n_o). \tag{2}$$

The s- and p-polarizations are chosen arbitrarily to align with the extraordinary (z-axis) and ordinary axes, respectively, within the poled polymer. The change in optical path difference is given by

$$\Delta(l_p - l_s) = d_s(\Delta n_e - \Delta n_o). \tag{3}$$

For simplicity, the values of the components are approximated as follows: $n = n_e \approx n_o$ and $\gamma_{33} = 3\gamma_{13}$, where γ_{33} and γ_{13} are the components of the EO tensor. Thus, the field-induced retardation in the proposed sensor can be expressed as follows.

We compare the proposed sensor (sensor 1) with the sensor with sandwich configurations (sensor 2) in terms of THz detection by EO sampling. The film of sensor 1 has a thickness of ~75 μm, whereas that of sensor 2 has a thickness of ~90 μm. The angle of incidence of sensor 2 is 60°, which is the Brewster's angle for PMMA-DR1 film. This angle is used because it provides the greatest probe beam transmission without significantly diminishing sensor efficiency. Using the theory developed (Eqs. (1), (4)) and the experimentally measured thicknesses (d_p, d_s), we obtain a measured refractive index of the optical probe beam with PMMA-DR1 of ≈1.6 at a wavelength of 800 nm and an incident angle of 60°. Thus, the ratio of the signal for the two sensors employed in our experiment should be

$$\frac{S_2}{S_1} \propto \frac{\Delta\Gamma_2}{\Delta\Gamma_1} \approx 1.67. \tag{4}$$

Figure 3 shows the THz electric field traces and the corresponding Fourier transforms using sensors 1 and 2. Over the detectable THz range, the measured ratios of the two sensors is only 70% of the predicted ratio of 1.67 because the electric field is assumed to be uniform throughout

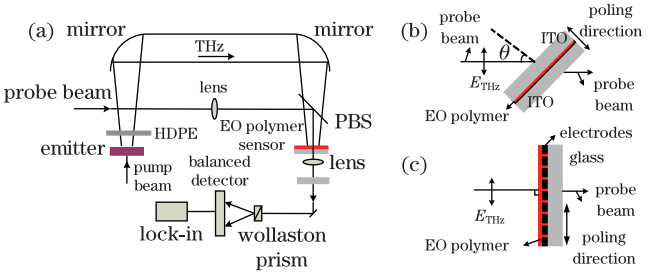

Fig. 2. (Color online) (a) Schematic of the experimental setup used in all-optical techniques. ZnTe is used to generate THz radiation by optical rectification and to detect THz radiation by EO sampling. PBS is a 2 μm pellicle beam splitter; (b) and (c) expanded view of the sensor on both sandwich and interdigitated coplanar configurations, respectively.

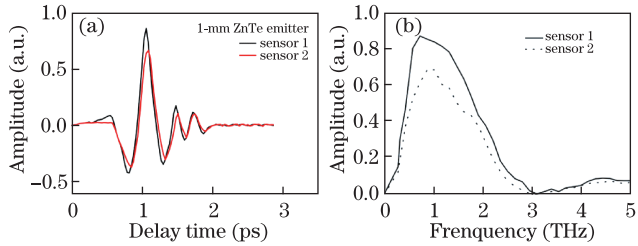

Fig. 3. (Color online) (a) Terahertz electric field traces for two sensors and (b) corresponding Fourier transforms. Sensor 2 is placed at an angle of 60°. A 1-mm ZnTe emitter is used in both cases. Data are obtained using the experimental setup described in Fig. 2(a).

both sensors when calculating the EO coefficient (γ_{33}). However, the electric field of sensor 1 is in fact non-uniform during the poling, resulting in a phase retardation ($\Delta\Gamma_2$) larger than the true value.

In conclusion, we report the application of EO polymers for THz sensing. Two configurations of EO polymer sensors are studied and compared in terms of their sensitivity as EO sensors. The proposed EO sensor with interdigitated coplanar electrodes more significantly improves sensitivity than does the sensor with sandwich configurations. Further studies should be conducted to elucidate the fundamental physics that governs the proposed sensor.

This work was supported by the National Natural Science Foundation of China (Nos. 60871073 and 61201075) and by China Postdoctoral Science Foundation (No. 2012M511507).

References

1. Q. Wu and X. C. Zhang, Appl. Phys. Lett. **68,** 1604 (1996).
2. A. Nahata, D. H. Auston, T. F. Heinz, and C. Wu, Appl. Phys. Lett. **68,** 150 (1996).
3. A. Nahata, D. H. Auston, C. Wu, and J. T. Yardley, Appl. Phys. Lett. **67,** 1358 (1995).
4. Y. Enami, C. T. Derose, D. Mathine, C. Loychik, C. Greenlee, R. A. Norwood, T. D. Kim, J. Luo, Y. Tian, A. K.-Y. Jen, and N. Peyghambarian, Nat. Photonics **1,** 180 (2007).
5. X. Piao, X. Zhang, Y. Mori, M. Koishi, A. Nakaya, S. Inoue, I. Aoki, A. Otomo, and S. Yokoyama, J. Poly. Sci. A: Poly. Chem. **49,** 47 (2011).
6. X. S .Cheng, W. W. Qiu, W. X. Wu, Y. H. Luo, X. J. Tian, Q. J. Zhang, and B. Zhu, Chin. Opt. Lett. **9,** 020602 (2011).
7. L. Wang, J. Liu, S. Bo, Z. Zhen, and X. Liu, Mater. Lett. **80,** 84(2012).
8. X. Zheng, A. Sinyukov, and L. M. Hayden, Appl. Phys. Lett. **87,** 081115 (2005).
9. Y. B. Jeon, R. Sood, J. Jeong, and S. G. Kim, Sens. Act. A: phys. **122,** 16(2005).
10. C. W. Christenson, C. Greenlee, B. Lynn, J. Thomas, P. A. Blanche, and N. Peyghambarian, Opt. Lett. **36,** 3377 (2011).
11. L. M. Hayden, A. M. Sinyukov, MR. Laehy, J. Fench, P. Gunter, W. N. Herman, R. J. Twieg, and H. Meng, J. Poly. Sci. B. **41,** 2492 (2003).
12. M. C. Gower, Opt. Express. **7,** 56 (2000).
13. A. Sandalphon, B. Kippelen, K. Meerholz, and N. Peyghambarian, Appl. Opt. **35,** 2346 (1996).
14. J. A. Valdmanis, G. Mourou, and C. W. Gabel, Appl. Phys. Lett. **41,** 211 (1982).
15. N. C. J. van der Valk, T. Wenckebach, and P. C. M. Planken, J. Opt. Soc. Am. B **21,** 622 (2004).
16. C. V. McLaughlin, X. Zheng, and L. M. Hayden, Appl. Opt. **25,** 6283 (2007).